OPTIMAL VARIABLE-STRUCTURE CONTROL TRACKING OF SPACECRAFT MANEUVERS

John L. Crassidis, Srinivas R. Vadali
Texas A&M University
Department of Aerospace Engineering
College Station, TX 77843-3141

F. Landis Markley
NASA-Goddard Space Flight Center
Guidance, Navigation, and Control Center, Code 571
Greenbelt, MD 20771

ABSTRACT

An optimal control approach using variable-structure (sliding-mode) tracking for large angle spacecraft maneuvers is presented. The approach expands upon a previously derived regulation result using a quaternion parameterization for the kinematic equations of motion. This parameterization is used since it is free of singularities. The main contribution of this paper is the utilization of a simple term in the control law that produces a maneuver to the reference attitude trajectory in the shortest distance. Also, a multiplicative error quaternion between the desired and actual attitude is used to derive the control law. Sliding-mode switching surfaces are derived using an optimal-control analysis. Control laws are given using either external torque commands or reaction wheel commands. Global asymptotic stability is shown for both cases using a Lyapunov analysis. Simulation results are shown which use the new control strategy to stabilize the motion of the Microwave Anisotropy Probe spacecraft.

INTRODUCTION

The control of spacecraft for large angle slewing maneuvers poses a difficult problem. Some of these difficulties include: the highly nonlinear characteristics of the governing equations, control rate and saturation constraints and limits, and incomplete state knowledge due to sensor failure or omission. The control of spacecraft with large angle slews can be accomplished by either open-loop or closed-loop schemes. Open-loop schemes usually require a pre-determined pointing maneuver and are typically determined using optimal control techniques, which involve the solution of a two-point boundary value problem (e.g., the time optimal maneuver problem[1]). Also, open-loop schemes are sensitive to spacecraft parameter uncertainties and unexpected disturbances.[2] Closed-loop systems can account for parameter uncertainties and disturbances, and thus provide a more robust design methodology.

In recent years, much effort has been devoted to the closed-loop design of spacecraft with large angle slews. Wie and Barba[3] derive a number of simple control schemes using quaternion and angular velocity (rate) feedback. Other full state feedback techniques have been developed that are based on variable-structure (sliding-mode) control, which uses a feedback linearizing technique and an additional term aimed at dealing with model uncertainty.[4] A variable-structure controller has been developed for the regulation of spacecraft maneuvers using a Gibbs vector parameterization,[5] a modified-Rodrigues parameterization,[6] and a quaternion parameterization.[7] In both [3] and [7], a term was added so that the spacecraft maneuver follows the shortest path and requires the least amount of control torque. The variable-structure control approach using a quaternion parameterization has been recently expanded to the attitude tracking case.[8,9] However, these controllers do not take into account the shortest possible

path as shown in Refs. [3] and [7]. This paper expands upon the results in Ref. [7] to provide an optimal control law for asymptotic tracking of spacecraft maneuvers using variable-structure control.

The organization of this paper proceeds as follows. First, the kinematic and dynamic equations of motion are summarized. Then, an analysis for the selection of the switching surfaces is shown. This is shown using both an optimal control approach and a Lyapunov stability-based approach. Also, variable-structure considerations will be investigated. Next, a variable-structure controller is derived using either external torque inputs or reaction wheels. Finally, simulation results will be shown which use the new control law to stabilize the motion of the Microwave Anisotropy Probe spacecraft.

BACKGROUND

In this section, a brief review of the kinematic and dynamic equations of motion for a three-axis stabilized spacecraft is shown. The attitude is assumed to be represented by the quaternion, defined as[10]

$$\boldsymbol{q} \equiv \begin{bmatrix} \boldsymbol{q}_{13} \\ q_4 \end{bmatrix} \tag{1}$$

with

$$\boldsymbol{q}_{13} \equiv \begin{bmatrix} q_1 \\ q_2 \\ q_3 \end{bmatrix} = \hat{\boldsymbol{n}} \sin(\Phi/2) \tag{2a}$$

$$q_4 = \cos(\Phi/2) \tag{2b}$$

where $\hat{\boldsymbol{n}}$ is a unit vector corresponding to the axis of rotation and Φ is the angle of rotation. The quaternion kinematic equations of motion are derived by using the spacecraft's angular velocity ($\boldsymbol{\omega}$), given by

$$\dot{\boldsymbol{q}} = \frac{1}{2}\Omega(\boldsymbol{\omega})\boldsymbol{q} = \frac{1}{2}\Xi(\boldsymbol{q})\boldsymbol{\omega} \tag{3}$$

where $\Omega(\boldsymbol{\omega})$ and $\Xi(\boldsymbol{q})$ are defined as

$$\Omega(\boldsymbol{\omega}) \equiv \begin{bmatrix} -[\boldsymbol{\omega}\times] & \vdots & \boldsymbol{\omega} \\ \cdots\cdots & \vdots & \cdots\cdots \\ -\boldsymbol{\omega}^T & \vdots & 0 \end{bmatrix} \tag{4a}$$

$$\Xi(\boldsymbol{q}) \equiv \begin{bmatrix} q_4 I_{3\times 3} + [\boldsymbol{q}_{13}\times] \\ \cdots\cdots\cdots\cdots\cdots \\ -\boldsymbol{q}_{13}^T \end{bmatrix} \tag{4b}$$

where $I_{n\times n}$ represents an $n\times n$ identity matrix (also, $0_{n\times m}$ will represent an $n\times m$ zero matrix). The 3×3 dimensional matrices $[\boldsymbol{\omega}\times]$ and $[\boldsymbol{q}_{13}\times]$ are referred to as cross product matrices since $\boldsymbol{a}\times\boldsymbol{b} = [\boldsymbol{a}\times]\boldsymbol{b}$, with

$$[\boldsymbol{a}\times] \equiv \begin{bmatrix} 0 & -a_3 & a_2 \\ a_3 & 0 & -a_1 \\ -a_2 & a_1 & 0 \end{bmatrix} \tag{5}$$

Since a three degree-of-freedom attitude system is represented by a four-dimensional vector, the quaternion components cannot be independent. This condition leads to the following normalization constraint

$$\boldsymbol{q}^T\boldsymbol{q} = \boldsymbol{q}_{13}^T\boldsymbol{q}_{13} + q_4^2 = 1 \tag{6}$$

The matrix $\Xi(\boldsymbol{q})$ obeys the following relations that are extremely useful

$$\Xi^T(\boldsymbol{q})\Xi(\boldsymbol{q}) = \boldsymbol{q}^T\boldsymbol{q}\, I_{3\times 3} \tag{7a}$$

$$\Xi(\boldsymbol{q})\Xi^T(\boldsymbol{q}) = \boldsymbol{q}^T\boldsymbol{q}\, I_{4\times 4} - \boldsymbol{q}\boldsymbol{q}^T \tag{7b}$$

$$\Xi^T(\boldsymbol{q})\boldsymbol{q} = \boldsymbol{0}_{3\times 1} \tag{7c}$$

$$\Xi^T(\boldsymbol{q})\boldsymbol{\zeta} = -\Xi^T(\boldsymbol{\zeta})\boldsymbol{q} \quad \text{for any } \boldsymbol{\zeta}_{4\times 1} \tag{7d}$$

$$\Xi^T(\boldsymbol{\zeta})\Xi(\boldsymbol{q}) = \left\{\left(\boldsymbol{q}^T\boldsymbol{\zeta}\right) I_{3\times 3} + \left[\Xi^T(\boldsymbol{\zeta})\boldsymbol{q}\times\right]\right\} \quad \text{for any } \boldsymbol{\zeta}_{4\times 1} \tag{7e}$$

Also, the error quaternion between two quaternions, $\boldsymbol{q}$ and $\boldsymbol{q}_d$, is defined by

$$\boldsymbol{\delta q} \equiv \begin{bmatrix} \boldsymbol{\delta q}_{13} \\ \hdashline \delta q_4 \end{bmatrix} = \boldsymbol{q} \otimes \boldsymbol{q}_d^{-1} \tag{8}$$

where the operator $\otimes$ denotes quaternion multiplication (see Ref. [10] for details), and the inverse quaternion is defined by

$$\boldsymbol{q}_d^{-1} = \begin{bmatrix} -q_{d_1} & -q_{d_2} & -q_{d_3} & q_{d_4} \end{bmatrix}^T \tag{9}$$

Other useful identities are given by

$$\boldsymbol{\delta q}_{13} = \Xi^T(\boldsymbol{q}_d)\boldsymbol{q} \tag{10a}$$

$$\delta q_4 = \boldsymbol{q}^T\boldsymbol{q}_d \tag{10b}$$

Also, if Equation (8) represents a small rotation then $\delta q_4 \approx 1$, and $\boldsymbol{\delta q}_{13}$ corresponds to half-angles of rotation.

The dynamic equations of motion, also known as Euler's equations, for a rotating spacecraft with are given by[11]

$$J\dot{\boldsymbol{\omega}} = -\boldsymbol{\omega}\times(J\boldsymbol{\omega}) + \boldsymbol{u} \tag{11}$$

where J is the inertia matrix of the spacecraft, and $\boldsymbol{u}$ is the total external torque input. If the spacecraft is equipped with 3 orthogonal reaction or momentum wheels, then Euler's equations become:

$$\left(J - \bar{J}\right)\dot{\boldsymbol{\omega}} = -\boldsymbol{\omega}\times\left(J\boldsymbol{\omega} + \bar{J}\bar{\boldsymbol{\omega}}\right) - \bar{\boldsymbol{u}} \tag{12a}$$

$$\bar{J}\left(\dot{\bar{\boldsymbol{\omega}}} + \dot{\boldsymbol{\omega}}\right) = \bar{\boldsymbol{u}} \tag{12b}$$

where $\bar{J}$ is the diagonal inertia matrix of the wheels, J now includes the mass of the wheels, $\bar{\boldsymbol{\omega}}$ is the wheel angular velocity vector, and $\bar{\boldsymbol{u}}$ is the wheel torque vector.

SELECTION OF SWITCHING SURFACES

Optimal Control Analysis

The variable-structure control design is used to track a desired quaternion $\boldsymbol{q}_d$ and corresponding angular velocity $\boldsymbol{\omega}_d$. As shown previously for regulation,[7] under ideal sliding conditions, the trajectory in the state-space moves on the sliding manifold. For tracking, the following loss function is minimized to determine the optimal switching surfaces:

$$\Pi(\boldsymbol{\omega}) = \frac{1}{2}\int_{t_s}^{\infty}\left[\rho\,\delta\boldsymbol{q}_{13}^{T}\delta\boldsymbol{q}_{13} + (\boldsymbol{\omega}-\boldsymbol{\omega}_d)^{T}(\boldsymbol{\omega}-\boldsymbol{\omega}_d)\right]dt \tag{13}$$

subject to the bilinear system constraint given in Equation (3). Note that ρ is a scalar gain and t_s is the time of arrival at the sliding manifold. Minimization of Equation (13) leads to the following two-point-boundary-value-problem:

$$\dot{\boldsymbol{q}} = \frac{1}{2}\Xi(\boldsymbol{q})\boldsymbol{\omega} \tag{14a}$$

$$\dot{\boldsymbol{\lambda}} = -\rho\,\Xi(\boldsymbol{q}_d)\Xi^{T}(\boldsymbol{q}_d)\boldsymbol{q} + \frac{1}{2}\Xi(\boldsymbol{\lambda})\boldsymbol{\omega} \tag{14b}$$

$$\boldsymbol{\omega}-\boldsymbol{\omega}_d = -\frac{1}{2}\Xi^{T}(\boldsymbol{q})\boldsymbol{\lambda} \tag{14c}$$

where $\boldsymbol{\lambda}$ is the co-state vector. The following sliding vector is chosen:

$$\boldsymbol{s} \equiv (\boldsymbol{\omega}-\boldsymbol{\omega}_d) + k\,\Xi^{T}(\boldsymbol{q}_d)\boldsymbol{q} = \boldsymbol{0} \tag{15}$$

where k is a scalar gain. The sliding vector is optimal if the solution of Equation (15) minimizes Equation (13). This can be proven by first substituting Equation (15) into Equation (14c) and using the matrix identities in Equation (7), yielding

$$\boldsymbol{\lambda} = -2\,k\,\boldsymbol{q}_d \tag{16}$$

Next, using the fact that the desired quaternion can be obtained from the following

$$\dot{\boldsymbol{q}}_d = \frac{1}{2}\Xi(\boldsymbol{q}_d)\boldsymbol{\omega}_d \tag{17}$$

leads directly to

$$\dot{\boldsymbol{\lambda}} = -k\,\Xi(\boldsymbol{q}_d)\boldsymbol{\omega}_d \tag{18}$$

Comparing Equation (18) to Equation (14b), and using Equation (15) now leads to the following relationship:

$$-k\,\Xi(\boldsymbol{q}_d)\boldsymbol{\omega}_d = -\rho\,\Xi(\boldsymbol{q}_d)\Xi^{T}(\boldsymbol{q}_d)\boldsymbol{q} - k\,\Xi(\boldsymbol{q}_d)\boldsymbol{\omega}_d + k^2\Xi(\boldsymbol{q}_d)\Xi^{T}(\boldsymbol{q}_d)\boldsymbol{q} \tag{19}$$

Equation (19) is satisfied for $k = \pm\sqrt{\rho}$. Therefore, the sliding condition in Equation (15) leads to an optimal solution (i.e., minimum Π in Equation (13)).

For this special case, it can be shown that the value of the loss function in Equation (13) is given by

$$\Pi^* = 2k\left[1 - \delta q_4(t_s)\right] \tag{20}$$

where k must now be strictly positive. Note that δq_4 corresponds directly to the cosine of half the angle error of rotation. Both $\boldsymbol{\delta q}$ and $-\boldsymbol{\delta q}$ represent the same rotation; however, the value of the loss function in Equation (20) is significantly different for each rotation. One rotation ($\boldsymbol{\delta q}$) gives the shortest distance to the sliding manifold, while the other ($-\boldsymbol{\delta q}$) gives the longest distance. Although each rotation gives the same orientation, more energy may be required to maneuver the spacecraft using $-\boldsymbol{\delta q}$. In order to give the shortest possible distance the following sliding vector is chosen:

$$\boldsymbol{s} \equiv (\boldsymbol{\omega} - \boldsymbol{\omega}_d) + k\,\mathrm{sgn}\left[\delta q_4(t_s)\right]\Xi^T(\boldsymbol{q}_d)\,\boldsymbol{q} = \boldsymbol{0} \tag{21}$$

where it is assumed that $\delta q_4(t_s)$ is non-zero for a finite time. Using this sliding condition leads to the following value for the loss function:

$$\Pi^* = 2k\left[1 - \left|\delta q_4(t_s)\right|\right] \tag{22}$$

which yields a minimal value for any rotation. The kinematic equation for δq_4 can now be written as

$$\dot{\delta q}_4 = \frac{1}{2}k\left(1 - \delta q_4^2\right)\mathrm{sign}\left[\delta q_4(t_s)\right] \tag{23}$$

Therefore, the derivative $\dot{\delta q}_4$ is either positive or negative depending on the sign of $\delta q_4(t_s)$, so the term $\mathrm{sgn}\left[\delta q_4(t_s)\right]$ can be replaced with $\mathrm{sgn}\left[\delta q_4(t - t_s)\right]$ without loss in generality (note, this corresponds to the time *after* the sliding manifold is reached).

Lyapunov Analysis

The sliding vector shown in Equation (21) can also be shown to be stable using a Lyapunov analysis. The time derivative of Equation (10a) can be shown to be given by

$$\dot{\boldsymbol{\delta q}}_{13} = \frac{1}{2}\delta q_4\,(\boldsymbol{\omega} - \boldsymbol{\omega}_d) + \frac{1}{2}\left[\boldsymbol{\delta q}_{13}\times\right](\boldsymbol{\omega} + \boldsymbol{\omega}_d) \tag{24}$$

Next, the following candidate Lyapunov function is chosen:

$$V_s = \frac{1}{2}\boldsymbol{\delta q}_{13}^T\boldsymbol{\delta q}_{13} \tag{25}$$

Using the sliding vector in Equation (21), the time derivative of Equation (25) is given by

$$\dot{V}_s = -\frac{1}{2}k\left|\delta q_4\right|\boldsymbol{\delta q}_{13}^T\boldsymbol{\delta q}_{13} \le 0 \tag{26}$$

Hence, V_s is indeed a Lyapunov function for $k > 0$. This analysis generalizes the results shown in Ref. [9], where the spacecraft's attitude is restricted in the workspace defined with $q_4 > 0$.

Sliding Manifold Considerations

The term $\mathrm{sgn}\left[\delta q_4(t_s)\right]$ is used to develop a control law that yields the shortest distance to the sliding manifold. However, in actual practice this manifold is difficult to visualize. This section shows an analysis for the optimality conditions during the transient response of the control design. The goal of the controller is to drive $\boldsymbol{s} \to \boldsymbol{0}$. Since the norm-squared of sliding vector is closely related to the energy of

the system, this can be useful to determine the optimal maneuver conditions for the spacecraft controller. Consider the following sliding vector:

$$\boldsymbol{s} = (\boldsymbol{\omega} - \boldsymbol{\omega}_d) + \psi\, \Xi^T(\boldsymbol{q}_d)\boldsymbol{q} \tag{27}$$

where ψ is some scalar (note: the sliding vector is now assumed to be non-zero). The following performance measure can be used to quantify how fast the sliding mode manifold is reached:

$$\frac{1}{2}\int_{t_0}^{t_1} \boldsymbol{s}^T\boldsymbol{s}\; dt = \frac{1}{2}\int_{t_0}^{t_1}\left[(\boldsymbol{\omega} - \boldsymbol{\omega}_d)^T(\boldsymbol{\omega} - \boldsymbol{\omega}_d) + \psi^2\delta\boldsymbol{q}_{13}^T\delta\boldsymbol{q}_{13} + 2\,\psi(\boldsymbol{\omega} - \boldsymbol{\omega}_d)^T\,\Xi^T(\boldsymbol{q}_d)\boldsymbol{q}\right]dt \tag{28}$$

where t_1 corresponds to the time to reach $\boldsymbol{s} = \boldsymbol{0}$. The integral in Equation (28) during the transient response should be evaluated in order to determine how various choices of ψ affect the transient response. However, a closed-form solution for the integral is extremely difficult to obtain in this case, since one now requires knowledge of the actual control inputs which affect the angular velocity and attitude. Still, a closed-form solution for the last term in Equation (28) can be found without this knowledge. The time derivative of Equation (10b) can be shown to be given by

$$\delta\dot{q}_4 = -\frac{1}{2}(\boldsymbol{\omega} - \boldsymbol{\omega}_d)^T\,\Xi^T(\boldsymbol{q}_d)\boldsymbol{q} \tag{29}$$

The last term in Equation (28) is now given by

$$\frac{1}{2}\int_{t_0}^{t_1}\left[2\,\psi(\boldsymbol{\omega} - \boldsymbol{\omega}_d)^T\,\Xi^T(\boldsymbol{q}_d)\boldsymbol{q}\right]dt = -2\,\psi\left[\delta q_4(t_1) - \delta q_4(t_0)\right] \tag{30}$$

Therefore, once a control has been determined then only the first two terms of the right-hand-side of Equation (28) need to be numerically determined. It will be shown through an analysis of the closed-form structure of Equation (29) that $\psi = k\,\mathrm{sgn}[\delta q_4(t)]$ should be used at all times (even before the sliding manifold is reached) in order to produce a response in the shortest distance. Equations (28) and (30) can be used to validate this approach from dynamic numerical simulations.

VARIABLE-STRUCTURE TRACKING

The goal of the variable-structure controller is to track a desired quaternion $\boldsymbol{q}_d$ and corresponding angular velocity $\boldsymbol{\omega}_d$. The variable-structure control design with external torques only is given by

$$\boldsymbol{u} = [\boldsymbol{\omega}\times]J\boldsymbol{\omega} + J\left\{\frac{1}{2}k\,\mathrm{sgn}(\delta q_4)\left[\Xi^T(\boldsymbol{q})\Xi(\boldsymbol{q}_d)\boldsymbol{\omega}_d - \Xi^T(\boldsymbol{q}_d)\Xi(\boldsymbol{q})\boldsymbol{\omega}\right] + \dot{\boldsymbol{\omega}}_d - G\,\boldsymbol{\vartheta}\right\} \tag{31}$$

where G is a 3×3 positive definite, diagonal matrix, and the i^{th} component of $\boldsymbol{\vartheta}$ is given by

$$\vartheta_i = \mathrm{sat}(s_i, \varepsilon_i), \qquad i = 1,2,3 \tag{32}$$

As stated previously, the term $\mathrm{sgn}(\delta q_4)$ is used to drive the system to the desired trajectory in the shortest distance. The saturation function is used to minimize chattering in the control torques. This function is defined by

$$\text{sat}(s_i,\varepsilon_i)\equiv\begin{cases}1 & \text{for} \quad s_i>\varepsilon_i \\ \dfrac{s_i}{\varepsilon} & \text{for} \quad |s_i|\le\varepsilon_i \\ -1 & \text{for} \quad s_i<-\varepsilon_i\end{cases} \qquad i=1,2,3 \tag{33}$$

where ε is a small positive quantity. Also, the sliding manifold is given by

$$\boldsymbol{s}=(\boldsymbol{\omega}-\boldsymbol{\omega}_d)+k\,\text{sgn}(\delta q_4)\Xi^T(\boldsymbol{q}_d)\boldsymbol{q} \tag{34}$$

The stability of the closed-loop system using this controller can be evaluated using the following candidate Lyapunov function

$$V=\frac{1}{2}\boldsymbol{s}^T\boldsymbol{s} \tag{35}$$

Using Equations (11), (31), and (34) the time-derivative of Equation (35) can be shown to be given by

$$\dot{V}=-\boldsymbol{s}^T G\boldsymbol{\vartheta} \tag{36}$$

which is always less than or equal to zero as long as G is positive definite.

If wheels are used to control the spacecraft, then the sliding mode controller is given by the following:

$$\bar{\boldsymbol{u}}=-[\boldsymbol{\omega}\times](J\boldsymbol{\omega}+\bar{J}\bar{\boldsymbol{\omega}})+(J-\bar{J})\left\{\frac{1}{2}k\,\text{sgn}(\delta q_4)\left[\Xi^T(\boldsymbol{q}_d)\Xi(\boldsymbol{q})\boldsymbol{\omega}-\Xi^T(\boldsymbol{q})\Xi(\boldsymbol{q}_d)\boldsymbol{\omega}_d\right]-\dot{\boldsymbol{\omega}}_d+G\boldsymbol{\vartheta}\right\} \tag{37}$$

The stability of the system can also be easily proven using the Lyapunov function in Equation (35).

Analysis

In this section an analysis of using $\text{sgn}(\delta q_4)$ for all times in the control law is shown. We first assume that the desired angular velocity is zero $(\boldsymbol{\omega}_d=\boldsymbol{0})$ and that the matrix G is given by a scalar times the identity matrix $(g\,I_{3\times3})$. We further assume that the thickness of the boundary layer ε and the gain g are sufficiently large so that

$$G\boldsymbol{\vartheta}=\beta\boldsymbol{\omega}+\beta k\,\text{sgn}(\delta q_4)\boldsymbol{\delta q}_{13} \tag{38}$$

where $\beta=g/\varepsilon$. Using Equations (11), (24), and (31), the closed-loop dynamics for $\boldsymbol{\omega}$ now become

$$\dot{\boldsymbol{\omega}}=-\frac{1}{2}k\,\text{sgn}(\delta q_4)\Xi^T(\boldsymbol{q}_d)\Xi(\boldsymbol{q})\boldsymbol{\omega}-\beta\boldsymbol{\omega}-\beta k\,\text{sgn}(\delta q_4)\boldsymbol{\delta q}_{13} \tag{39}$$

Next, using Equation (7e) with $\boldsymbol{\zeta}=\boldsymbol{q}_d$ leads directly to

$$\dot{\boldsymbol{\omega}}=-\frac{1}{2}k\,\text{sgn}(\delta q_4)\left\{\delta q_4 I_{3\times3}+[\boldsymbol{\delta q}_{13}\times]\right\}\boldsymbol{\omega}-\beta\boldsymbol{\omega}-\beta k\,\text{sgn}(\delta q_4)\boldsymbol{\delta q}_{13} \tag{40}$$

Taking the time derivative of Equation (29), and using both Equation (40) and the quaternion constraint equation yield

$$\delta\ddot{q}_4+\left(\frac{1}{2}k|\delta q_4|+\beta\right)\delta\dot{q}_4+\left(\frac{1}{2}\beta k|\delta q_4|+\frac{1}{4}\boldsymbol{\omega}^T\boldsymbol{\omega}\right)\delta q_4=\frac{1}{2}\beta k\,\text{sgn}(\delta q_4) \tag{41}$$

Equation (41) represents a second-order nonlinear spring-mass-damper type system with an exogenous step input. The stability of Equation (41) can be evaluated by considering the following candidate Lyapunov function

$$V_{\delta q_4} = \frac{1}{2}\delta\dot{q}_4^2 + \frac{1}{2}\left(\frac{1}{4}\boldsymbol{\omega}^T\boldsymbol{\omega}\right)\delta q_4^2 + \frac{1}{2}\beta k\left[1 - \delta q_4 \operatorname{sgn}(\delta q_4)\right] \tag{42}$$

Also, the last term in Equation (41) is always greater or equal to zero since $\beta > 0$, $k > 0$, and $0 \le \delta q_4 \operatorname{sgn}(\delta q_4) \le 1$. Next, we assume that δq_4 is non-zero for a finite time. This is a valid assumption since the control law is known to produce asymptotic tracking in the closed-loop attitude response. Therefore, taking the time-derivative of Equation (42), and using Equations (40) and (41) give

$$\dot{V}_{\delta q_4} = -\left(\frac{1}{2}k|\delta q_4| + \beta\right)\delta\dot{q}_4^2 - \frac{1}{4}\left(\beta + \frac{1}{2}k|\delta q_4|\right)\left(\boldsymbol{\omega}^T\boldsymbol{\omega}\right)\delta q_4^2 \tag{43}$$

Hence, since $\beta > 0$ and $k > 0$, Equation (42) is indeed a Lyapunov function. The advantage of using $\operatorname{sgn}(\delta q_4)$ in the control law at all times (even before the sliding manifold is reached) now becomes clear. The step input in Equation (40) is a function of $\operatorname{sgn}(\delta q_4)$. Therefore, the response for δq_4 will approach $\operatorname{sgn}(\delta q_4)$ for any initial condition. This tends to drive the system to the desired location in the shortest distance. Furthermore, this inherently takes into account the rate errors as well. For example say that $\delta q_4(t_0)$ is positive, and that a high initial rate is given which tends to drive the system away from $\delta q_4 = 1$. The control law will automatically begin to null the rate. But, if the initial rate is large enough and the control dynamics are relatively slow, then δq_4 may become negative. Since $\operatorname{sgn}(\delta q_4)$ is used in the control system, then from Equation (40) the control law will subsequently drive the system towards $\delta q_4 = -1$. Therefore, using $\operatorname{sgn}(\delta q_4)$ at all times produces an optimal response for any type of initial condition error.

Robustness

In this section the robustness of the variable-structure controller with respect to modeling errors and external disturbances is addressed. This closely follows the approaches shown in Ref. [12]. We first define the following bounded modeling errors for the inertia matrix:

$$J = \hat{J} + \Delta J \tag{44a}$$

$$J^{-1} = \hat{J}^{-1} + \delta J \tag{44b}$$

where $\hat{J}$ is the nominal inertia matrix. Next, neglecting the gyroscopic term in Euler's equations, and adding an external disturbance input yields

$$\dot{\boldsymbol{\omega}} = J^{-1}\boldsymbol{u} + J^{-1}\boldsymbol{d} \tag{45}$$

where $\boldsymbol{d}$ denotes a bounded disturbance input. Under these conditions the time-derivative of the sliding manifold can be approximated by

$$\dot{\boldsymbol{s}} \approx \delta J\hat{J}\left\{\frac{1}{2}k\operatorname{sgn}(\delta q_4)\left[\Xi^T(\boldsymbol{q})\Xi(\boldsymbol{q}_d)\boldsymbol{\omega}_d - \Xi^T(\boldsymbol{q}_d)\Xi(\boldsymbol{q})\boldsymbol{\omega}\right] + \dot{\boldsymbol{\omega}}_d - G\boldsymbol{\vartheta}\right\} - J^{-1}\hat{J}G\boldsymbol{\vartheta} + J^{-1}\boldsymbol{d} \tag{46}$$

where it is assumed that the higher-order perturbations in the inertia matrix are small. Also, we again assume that the thickness of the boundary layer ε and the gain G are sufficiently large to keep the time

derivative of the associated Lyapunov function negative-definite with modeling errors and external disturbances. Then the dynamics of the sliding manifold reduce down to

$$\dot{\boldsymbol{s}} \approx -\frac{1}{\varepsilon} J^{-1} \hat{J} G \boldsymbol{s} + J^{-1} \boldsymbol{d} \tag{47}$$

Therefore, if the time derivative of the sliding manifold is small after all transients have decayed, then $\boldsymbol{s}$ will satisfy the following inequality

$$\|\boldsymbol{s}\| \le \left\| \varepsilon \left(\hat{J} G \right)^{-1} \right\| \|\boldsymbol{d}\|_{\max} \tag{48}$$

Equation (48) is valid using either external torques or reaction wheels in the control system.

ATTITUDE CONTROL OF MAP

In this section, the variable-structure controller is used to control the attitude of the Microwave Anisotropy Probe (MAP) spacecraft from quaternion observations and gyro measurements. The spacecraft is due to be launched around the year 2000. The objective of the MAP mission is to create a full-sky map of the cosmic microwave background and measure anisotropy with 0.3° angular resolution, in order to answer fundamental cosmological questions such as, inflationary versus non-inflationary "big bang" models, accurate determination of the Hubble constant, and the existence and nature of dark matter.

The ideal orbit for the MAP spacecraft is about the Earth-Sun L_2 Lagrange point, which is a Lissajous orbit with approximately a 180-day period. Because of its distance, 1.5 million km from Earth, this orbit affords great protection from the Earth's microwave emission, magnetic fields, and other disturbances, with the dominant disturbance torque being solar radiation pressure. It also provides for a very stable thermal environment and near 100% observing efficiency, since the Sun, Earth, and Moon are always behind the instrument's field of view. In this orbit MAP sees a Sun/Earth angle between 2 and 10 degrees. The instrument scans an annulus in the hemisphere away from the Sun, so the universe is scanned twice as the Earth revolves once around the sun.

The spacecraft orbit and attitude specifications are shown in Figure 1. To provide the scan pattern, the spacecraft spins about the z-axis at 0.464 rpm, and the z-axis cones about the Sun-line at 1 rev/hour. A 22.5°±0.25° angle between the z-axis and the Sun direction must be maintained to provide a constant power input, and to provide constant temperatures for alignment stability and science quality. The instrument pointing knowledge is 1.8 arcmin (1σ), which is not required for onboard or real-time implementation.

The spacecraft's attitude is defined by a 3-1-3 Euler angle rotation relative to a rotating, Sun-referenced frame. The three Euler angles are ϕ_d, θ_d, and ψ_d, and the desired states for observing mode are

$$\dot{\phi}_d = 1 \frac{\text{rev}}{\text{hr}} = 0.001745 \frac{\text{rad}}{\text{sec}} \tag{49a}$$

$$\theta_d = 22.5° = 0.3927 \text{rad} \tag{49b}$$

$$\dot{\psi}_d = 0.464 \text{ rpm} = 0.04859 \frac{\text{rad}}{\text{sec}} \tag{49c}$$

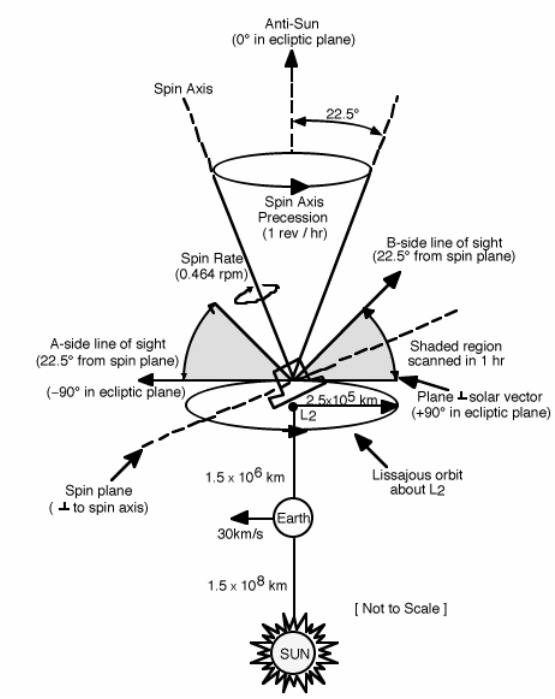

Fig. 1 MAP Spacecraft Specifications

The desired Euler angles for ϕ_d and ψ_d are determined by integrating the Euler rates. Also, $\dot{\theta}_d$ is set to zero. The commanded quaternion is determined using

$$q_{d_1} = \sin\left(\frac{\theta_d}{2}\right)\cos\left(\frac{\phi_d - \psi_d}{2}\right) \tag{50a}$$

$$q_{d_2} = \sin\left(\frac{\theta_d}{2}\right)\sin\left(\frac{\phi_d - \psi_d}{2}\right) \tag{50b}$$

$$q_{d_3} = \cos\left(\frac{\theta_d}{2}\right)\sin\left(\frac{\phi_d + \psi_d}{2}\right) \tag{50c}$$

$$q_{d_4} = \cos\left(\frac{\theta_d}{2}\right)\cos\left(\frac{\phi_d + \psi_d}{2}\right) \tag{50d}$$

The kinematic equation that transforms the commanded Euler rates to the commanded body rates is given by

$$\boldsymbol{\omega}_d = \begin{bmatrix} \sin\theta_d \sin\psi_d & \cos\psi_d & 0 \\ \sin\theta_d \cos\psi_d & -\sin\psi_d & 0 \\ \cos\theta_d & 0 & 1 \end{bmatrix} \begin{bmatrix} \dot{\phi}_d \\ \dot{\theta}_d \\ \dot{\psi}_d \end{bmatrix} \tag{51}$$

A number of simulation studies have been performed in order to test the variable-structure controller performance. The first test case involves a slewing maneuver using the following initial condition for the actual quaternion:

$$\boldsymbol{q}(t_0) = \begin{bmatrix} 0 & 0 & \sin(\Phi/2) & \cos(\Phi/2) \end{bmatrix}^T \otimes \boldsymbol{q}_d(t_0) \tag{52}$$

where the angle of rotation error has been set to $\Phi = 60^\circ$. Also, the actual angular velocity has been set to the desired angular velocity. This case uses external torques to maneuver the spacecraft. The control system has been designed to bring the actual attitude to the desired attitude in less than 20 minutes. The gains used in the control law are: $k = 0.015$, $G = 0.0015\, I_{3\times 3}$, and $\varepsilon = 0.01$. A plot of the roll, pitch, and yaw attitude errors are shown in Figure 2. Clearly, the control system achieves the desired performance. Plots of the angular velocity errors and control torques are shown in Figures 3 and 4, respectively. The sinusoidal components of the control torques in the X and Y axes are used to achieve the desired spin motion.

The next case shows how using $k\,\mathrm{sgn}\left[\delta q_4(t)\right]$ in the variable-structure controller achieves an optimal response (i.e., in the shortest distance). For this case, the initial attitude is given using Equation (52) with $\Phi = 60^\circ$ again. However, a large initial angular velocity error has been introduced, with $\boldsymbol{\omega}(t_0) = -5\,\boldsymbol{\omega}_d(t_0)$. This tends to drive the spacecraft in the opposite direction of the desired attitude. A plot of $\delta q_4(t)$ using $k\,\mathrm{sgn}\left[\delta q_4(t)\right]$ (solid line) in the controller and $\delta q_4(t)$ using just k (dotted line) in the controller, analogous to the approach in [8] and [9], is shown in Figure 5. Clearly, using $k\,\mathrm{sgn}\left[\delta q_4(t)\right]$ in the variable-structure controller achieves a faster response with less transients. This is also shown in the angular velocity responses, shown in Figures 6 and 7. Also, a plot comparing the magnitudes of the control inputs using $k\,\mathrm{sgn}\left[\delta q_4(t)\right]$ (solid line) and using k (dotted line) is shown in Figure 8. Using $k\,\mathrm{sgn}\left[\delta q_4(t)\right]$ results in a 22% reduction (root-mean-square) in the control effort to achieve the desired reference attitude and angular velocity.

To further illustrate the importance of using $k\,\mathrm{sgn}\left[\delta q_4(t)\right]$, a number of other simulations have been run for a rest-to-rest maneuver with the desired attitude set to the identity quaternion, and the desired angular velocity set to zero. The initial actual velocity has also been set to zero, and the initial quaternion has been computed using Equation (52). Test cases have been executed using $\Phi = 210^\circ$, 240°, 270°, 300°, and 330°. For all these test cases the spacecraft has been controlled using reaction wheels. A plot of the $\left(\delta\dot{q}_4, \delta q_4\right)$ phase plane is shown in Figure 9 (solid lines correspond to using $k\,\mathrm{sgn}\left[\delta q_4(t)\right]$ and dotted lines correspond to using k in the controller). Although not shown here, the response is the same for $0^\circ < \Phi < 180^\circ$. However, using $k\,\mathrm{sgn}\left[\delta q_4(t)\right]$ produces a response that is always optimal for any rotation error angle. Equation (28) has also been evaluated for each Φ used in this simulation. Table 1 summarizes the results for $k\,\mathrm{sgn}\left[\delta q_4(t)\right]$ and just k only. Clearly, by using $k\,\mathrm{sgn}\left[\delta q_4(t)\right]$ in the control law, better performance is achieved in the closed-loop system than using just k. This again shows that $k\,\mathrm{sgn}\left[\delta q_4(t)\right]$ is important in the variable-structure controller.

The final simulation shows how Equation (48) can be used to bound the steady-state errors. For this simulation the following external disturbance has been added:

$$\boldsymbol{d} = \begin{bmatrix} 0.005\sin(0.05t) \\ 0.003 \\ 0.005\cos(0.05t) \end{bmatrix} \tag{53}$$

A plot of the sliding manifold $\boldsymbol{s}$ and associated bound using Equation (48) is shown in Figure 10. This clearly shows the effectiveness of Equation (48) to accurately bound the sliding manifold errors.

Table 1 Cost Function Values for Various Φ

	Value of $\frac{1}{2}\int_{t_0}^{t_1} \boldsymbol{s}^T \boldsymbol{s}\, dt$	
Φ (deg)	k case	$k\,\mathrm{sgn}[\delta q_4(t)]$ case
210	1.0787	0.9313
240	0.8988	0.6543
270	0.6136	0.3566
300	0.3185	0.1300
330	0.1095	0.0194

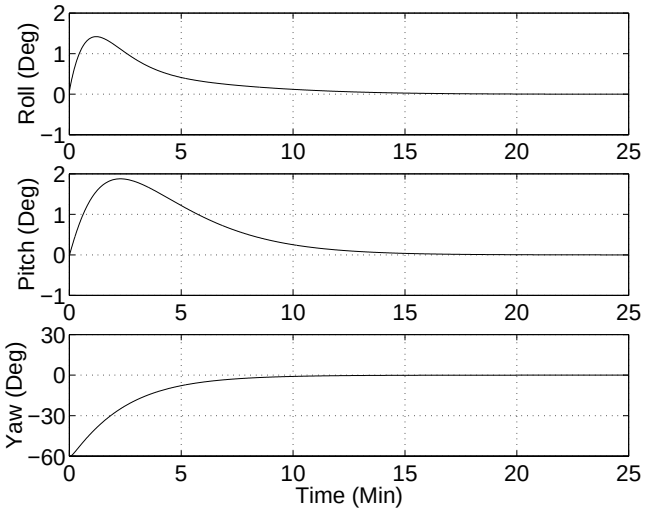

Fig. 2 Attitude Angle Errors

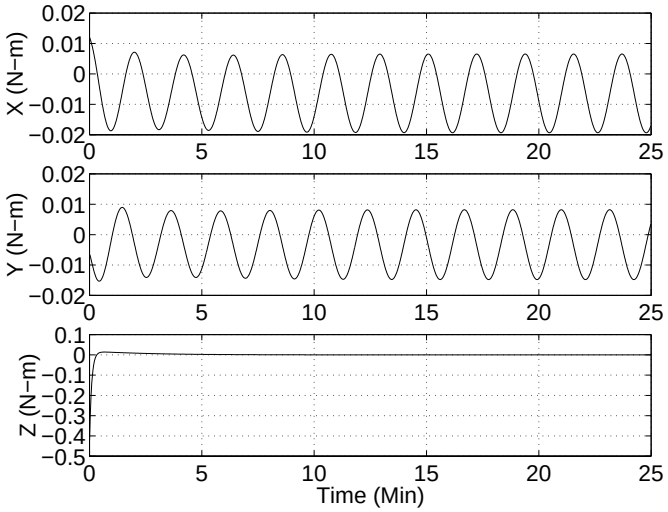

Fig. 4 Control Torque Inputs

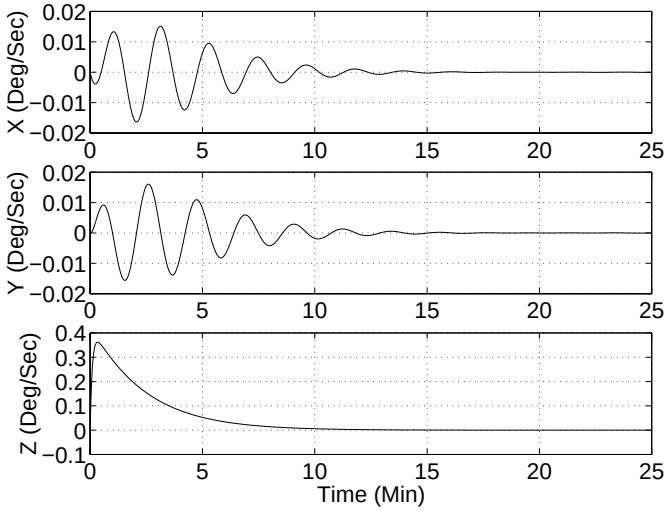

Fig. 3 Angular Velocity Errors

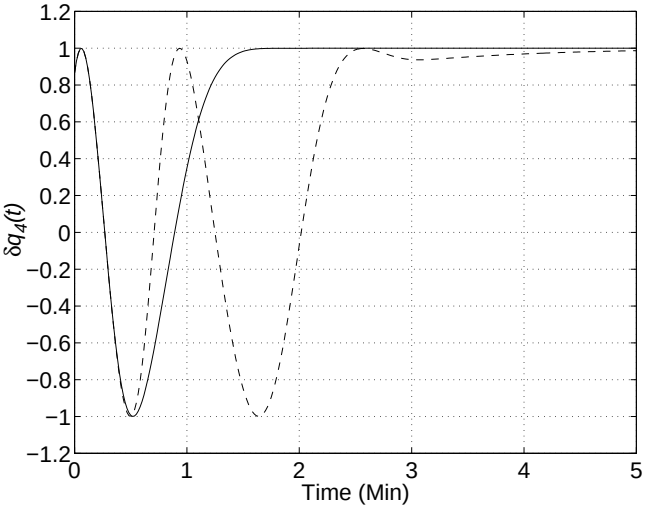

Fig. 5 Optimal (solid line) and Non-Optimal (dotted line) Error Quaternion Comparison

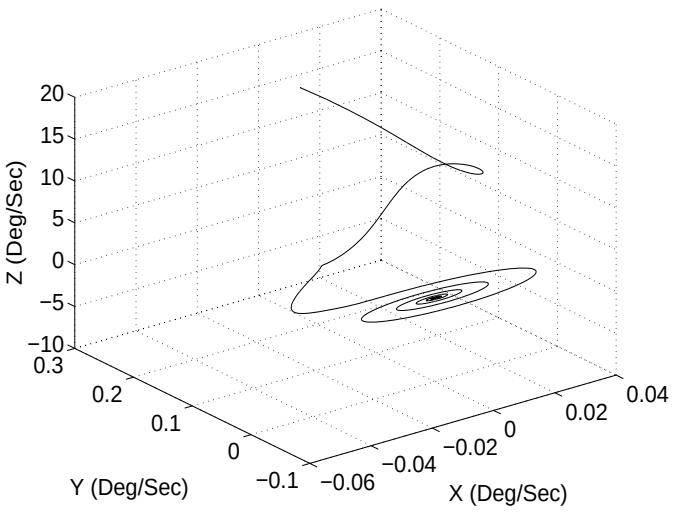

Fig. 6 Non-Optimal Angular Velocity Response

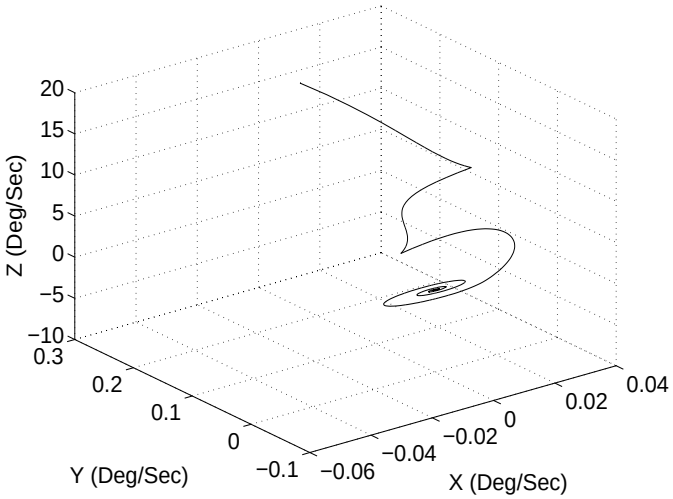

Fig. 7 Optimal Angular Velocity Response

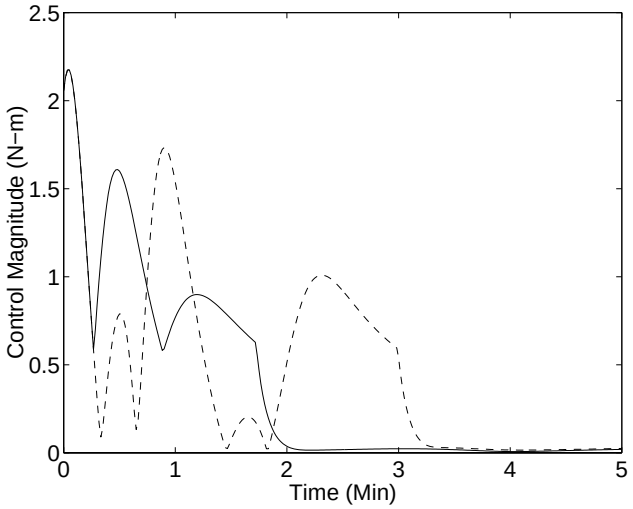

Fig. 8 Optimal (solid line) and Non-Optimal (dotted line) Control Input Magnitude Comparison

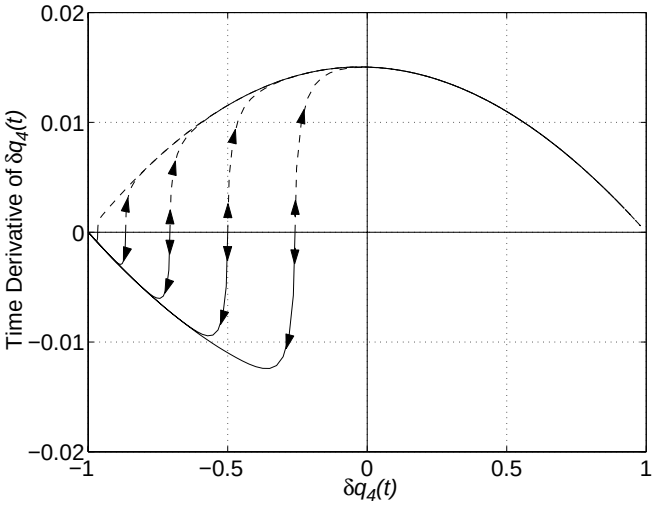

Fig. 9 Phase Portrait Plot

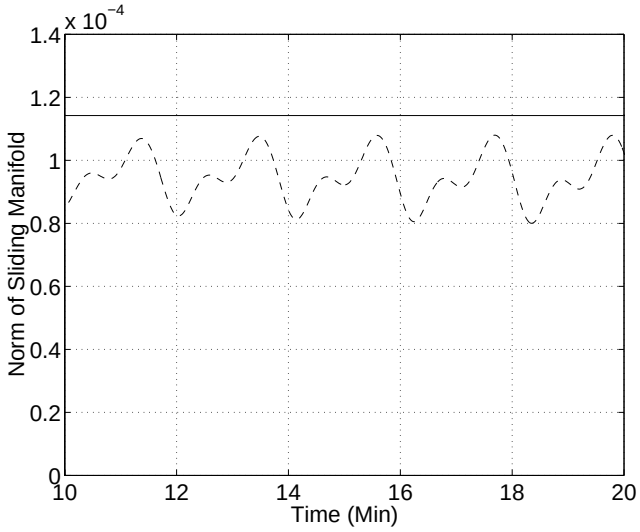

Fig. 10 Norm of the Sliding Manifold and Upper Bound

CONCLUSIONS

A new variable-structure controller for optimal spacecraft tracking maneuvers has been shown. The new controller was formulated for both external torque inputs and reaction wheel inputs. Global asymptotic stability was shown using a Lyapunov analysis. A simple term in the control law was used to produce a maneuver to the reference attitude trajectory in the shortest distance. The sliding motion was shown to be optimal in the sense of a quadratic loss function in the multiplicative error quaternions and angular velocities. A simulation study was performed which uses the new control law to stabilize the motion of the Microwave Anisotropy Probe spacecraft. Results indicated that the addition of the simple term in the control law always provides an optimal response, so that the reference attitude motion is achieved in the shortest possible distance.

REFERENCES

[1] Scrivener, S.L., and Thompson, R.C., "Survey of Time-Optimal Attitude Maneuvers," *Journal of Guidance, Control and Dynamics*, Vol. 17, No. 2, March-April 1994, pp. 225-233.

[2] Vadali, S.R., and Junkins, J.L., "Optimal Open-Loop and Stable Feedback Control of Rigid Spacecraft Maneuvers," *The Journal of the Astronautical Sciences*, Vol. 32, No. 2, April-June 1984, pp. 105-122.

[3] Wie, B., and Barba, P.M., "Quaternion Feedback for Spacecraft Large Angle Maneuvers," *Journal of Guidance*, Vol. 8, No. 3, May-June 1985, pp. 360-365.

[4] Slotine, J.J.E., and Li, W., *Applied Nonlinear Control*, Prentice Hall, NJ, 1991.

[5] Dwyer, T.A.W., and Sira-Ramirez, H., "Variable Structure Control of Spacecraft Reorientation Maneuvers," *Journal of Guidance, Control and Dynamics*, Vol. 11, No. 3, May-June 1988, pp. 262-270.

[6] Crassidis, J.L., and Markley, F.L., "Sliding Mode Control Using Modified Rodrigues Parameters," *Journal of Guidance, Control and Dynamics*, Vol. 19, No. 6, Nov.-Dec. 1996, pp. 1381-1383.

[7] Vadali, S.R., "Variable-Structure Control of Spacecraft Large-Angle Maneuvers," *Journal of Guidance, Control and Dynamics*, Vol. 9, No. 2, March-April 1986, pp. 235-239.

[8] Robinett, R.D., and Parker, G.G., "Least Squares Sliding Mode Control Tracking of Spacecraft Large Angle Maneuvers," *Journal of the Astronautical Sciences*, Vol. 45, No. 4, Oct.-Dec. 1997, pp. 433-450.

[9] Lo, S.-C., and Chen, Y.-P., "Smooth Sliding-Mode Control for Spacecraft Attitude Tracking Maneuvers," *Journal of Guidance, Control and Dynamics*, Vol. 18, No. 6, Nov.-Dec. 1995, pp. 1345-1349.

[10] Shuster, M.D., "A Survey of Attitude Representations," *The Journal of the Astronautical Sciences*, Vol. 41, No. 4, Oct.-Dec. 1993, pp. 439-517.

[11] Markley, F.L., "Equations of Motion," *Spacecraft Attitude Determination and Control*, Wertz, J.R., (editor), Kluwer Academic Publishers, Dordrecht, 1978, pp. 521-523.

[12] Kim, J., and Crassidis, J.L., "A Comparative Study of Sliding Mode Control and Time-Optimal Control," *Proceedings of the AIAA/AAS Astrodynamics Specialist Conference,* Boston, MA, Aug. 1998, AIAA Paper #98-4473.